Phase Separation Behavior of Silicate Phases Grown in Poly(methyl methacrylate) by a Sol−Gel Process

D. E. Rodrigues, B. G. Risch, and G. L. Wilkes*

Department of Chemical Engineering, Polymer Materials and Interfaces Laboratory, Virginia Polytechnic Institute and State University, Blacksburg, Virginia 24061-0211

Received October 30, 1996. Revised Manuscript Received July 31, 1997[⊗]

The diffusion and growth of an inorganic phase, namely, silica (obtained by reacting tetraethyl orthosilicate) in poly(methyl methacrylate) (PMMA), has been studied using small-angle X-ray scattering as well as electron microscopy. Previous workers have documented some of the structural features as well as the mechanical properties of such a composite system. In this work an emphasis has been placed on the fractal characteristics of the microscopic particles observed utilizing small-angle X-ray scattering. Fractal characteristics of the silica particles have been studied while varying the tetraethyl orthosilicate content with respect to PMMA. The growth of these particles in PMMA was also studied as a function of the reaction media. Typically, the silica forms mass fractals when reacted in a solvent media of tetrahydrofuran. When a small amount of dimethylformamide is added to the reaction, the fractal dimension varies from surface to mass fractal depending upon metal alkoxide content.

Introduction

For several years, silicate-based materials have been prepared utilizing the sol−gel route. The classical sol−gel process involves a series of chemical reactions that together convert the soluble metal or semimetal alkoxide into a ceramic at a relatively low temperature. Metal alkoxides such as tetraethyl orthosilicate (TEOS) and tetramethyl orthosilicate (TMOS) are easily catalyzed using either acidic or basic catalysts and will undergo the sol−gel reaction . The catalyst, either an acid or a base, strongly influences the reaction kinetics as well as the final gel structure.[1] A general representation of the sol gel reactions is given in Scheme 1 for the most commonly studied of metal alkoxides, i.e., TEOS. Since water is incompatible with TEOS, a solvent such as an alcohol, tetrahydrofuran (THF), or *N*, *N*-dimethylformamide (DMF) is used to obtain a homogeneous reaction mixture. Solvents can be protic, aprotic, polar, etc., and their role in the sol−gel process can greatly vary as a function of the pH of the reaction solution. In brief, the metal alkoxide first undergoes a hydrolysis reaction in which the alkoxide group (OR) is replaced with hydroxyl groups (OH). The SiOH or silanol then undergoes self-condensation or attacks an as yet unhydrolyzed alkoxide moiety to produce polymeric silica (Si−O−Si) plus the corresponding alcohol (ROH) or water as indicated by the reactions in Scheme 1. In most cases the condensation reaction proceeds before the hydrolysis reaction is over.[1] The relative rate of condensation with respect to the hydrolysis will not only have a decisive influence on the network forming process, but also have an influence on the completeness of the hydrolysis. This complication has made the sol−gel process one of the most difficult to understand and control. The effect of various catalysts as well as solvents on the reaction as well as the resulting structure of the silicate particles produced has been studied and documented.[2−5] As stated above, these studies indicate that the nature of the reaction as well as the reaction products are sensitive to the conditions of the reaction.

Scheme 1

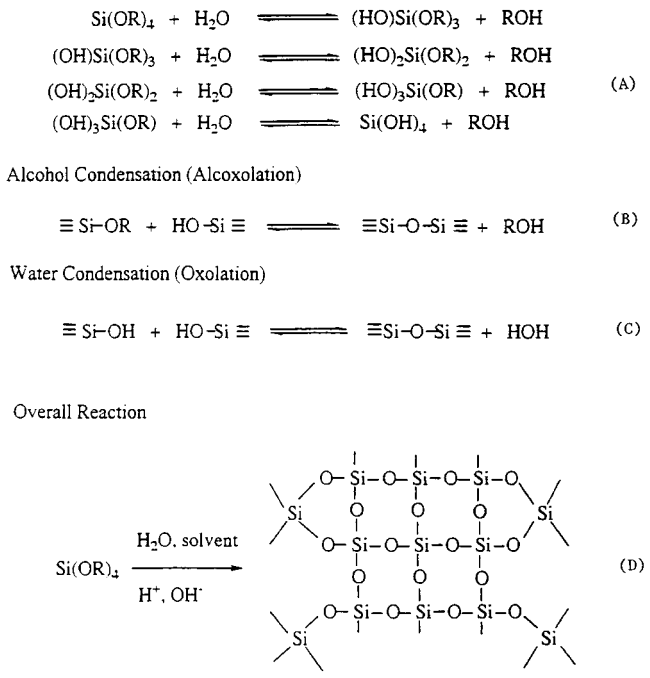

The sol gel approach has also been utilized to grow inorganic particles in an organic matrix thereby produc-

* To whom correspondence should be addressed.

[⊗] Abstract published in *Advance ACS Abstracts,* October 15, 1997.

(1) Brinker, C. J.; Scherer, G. W. Sol Gel Science. In *The Physics and Chemistry of Sol Gel Processing;* Academic Press, Inc.: San Diego, CA, 1990.

(2) Aelion, R.; Loebel, A; Eirich, F. *J. Am. Chem. Soc.* **1950**, *72*, 5705.

(3) Keefer, K. D. *Mater. Res. Soc. Symp. Proc.* **1984**, *32*, 15.

(4) Zerda, T. W.; Artaki, I.; Jonas, J. *J. Non-Cryst. Solids.* **1986**, *81*, 365.

(5) Artaki, I.; Bradley, M.; Zerda, T. W.; Jonas, J. *J. Phys. Chem.* **1985**, *89*, 4399.

S0897-4756(96)00562-5 CCC: $14.00

ing new materials with properties that may possess some characteristics intermediate between that of the matrix and the inorganic components. Over the past few years, several different approaches have been employed to achieve this objective. Mark et al.[6−9] showed that it was possible to "fill" already cured networks of poly(dimethylsiloxane) (PDMS) with TEOS and subsequently in situ hydrolyze the monomer in an aqueous solution of acid, base, or salt as catalyst. Silica particles of size 200 Å were found to be precipitated in the siloxane network as evidenced from transmission electron microscopy, and some of the ultimate properties of the network were significantly improved.[10] Small-angle X-ray scattering (SAXS) and small-angle neutron scattering (SANS) were conducted on these materials in order to study the structure of the silicate particles.[11] These studies revealed the silicate particles to be compact with sharp interfaces when acid catalysis was used. When base catalysis was used, the interface, however, varied from diffuse to sharp as TEOS content was reduced. The authors also reported the presence of large scale structure in the networks shortly after catalyst introduction. These larger structures are produced as a result of incompatibility between TEOS and PDMS.

More recently Wilkes and co-workers have coreacted metal alkoxides such as TEOS, TMOS, titanium(IV) isopropoxide (TiOPr), and zirconium *n*-isopropoxide (ZrOPr) with triethoxysilane end-functionalized organics such as poly(tetramethylene oxide) (PTMO), polyetherketone (PEK), polysulfone (PSF), polyimide (PI) etc.,[12−17] thereby imparting some very useful properties such as improvements in refractive index[18] and mechanical properties .[19] Structural studies using SAXS were also conducted on hybrid inorganic−organic materials produced by reacting TEOS with isocyanatopropyltriethoxysilane endcapped PTMO in cosolvent systems of THF−2-propanol (IPA) and DMF−IPA.[20,21] From these studies it was found that, when a functionalized oligomer of molecular weight of 2000 g/mol was used, microphase separation between the silicate and the PTMO produced an interparticle interference SAXS peak signifying an interdomain spacing of ca. 100 Å, which was found to increase with metal alkoxide content. The interdomain spacing and hence the interparticle interference peak was also found to be dependent upon the molecular weight of the organic spacer. The SAXS profiles were further subjected to analysis in the Guinier and Porod regions from which it was found that the silicate particles produced as a result of the reaction in THF−IPA were mass fractals for all initial weight fractions of TEOS−PTMO.[21] In the case of the reaction conducted in DMF−IPA, the structure of the scattering particle was found to be dependent upon the initial ratio of TEOS to PTMO. At low TEOS weight fractions the silicate particles showed mass fractal behavior, while at higher weight fractions (above 40 wt %) they showed surface fractal behavior. This was attributed to the DMF which has a more alkaline nature and also promotes phase separation of the silicate from the PTMO.

Landry and co-workers[22,23] have more recently pioneered the development of in situ silicate particles by catalyzing TEOS in an organic matrix of poly(methyl methacrylate) (PMMA), poly(vinyl acetate) (PVAc), poly(vinylpyrrolidone) (PVP), or poly(methyl methacrylate-*co*-methacrylic acid) (10 mol % MAA) PMMA-*co*-MAA) containing no functional groups. While strong secondary bonding was promoted, no direct primary covalent bonding was expected between the inorganic and the organic components. In the case of the TEOS−PMMA system specifically, the authors performed dynamic mechanical analysis on the composite and determined that, when an acid catalyst was used, the silicate component was found to act as a binder and provide reinforcement to the matrix such that the storage modulus (G') plateau of the composite system extended up to 250 °C. The type of particles developed in these systems was found to be dependent upon the nature of the catalyst and this consequently determines the interactions between the silicate particles and the PMMA matrix. Strong hydrogen-bonding interactions were suggested to be the principal factor in determining whether a homogeneous system of silicate and organic was formed.[23]

In a more recent report, Landry and co-workers[24] proposed two SAXS morphological models to describe scattering for inorganic organic materials. These studies were conducted on triethoxysilane endcapped bisphenol A epoxide (EAS) resin reacted in the presence of TEOS under slightly basic conditions and a random trimethoxysilane-functionalized copolymer of poly(methyl methacrylate) with added tetramethoxysilane (MMA−TMS) reacted in an acidic medium. Both materials displayed a broad scattering maxima and a limiting high angle slope commonly seen in SAXS profiles. The authors conclude that, for the MMA−TMS system, particulate growth occurs as a result of spinodal decomposition and that the composite is better described by bicontinuous inorganic−organic phases with a mean separation of 40 Å. In the case of the EAS hybrid, the composite exhibits particle characteristics at length scales smaller than 250 Å, while at larger distances the inorganic and organic phases are bicontinuous. In view

(6) Jiang, C.-Y.; Mark, J. E. ,*Makromol. Chem.* **1984**, *185*, 2609.
(7) Mark, J. E.; Ning, Y. P. *Polym. Bull.* **1984**, *12*, 413.
(8) Mark, J. E.; Sun, C.-C. *Polym. Bull.* **1985**, *18*, 259.
(9) Clarson, J.; Mark, J. E. *Polym. Commun.* **1987**, *28*, 249.
(10) Mark, J. E.; Ning, Y.-P.; Jiang, C.-Y.; Tang, M.-Y.; Roth, W. C. *Polymer* **1985**, *26*, 2069.
(11) Schaefer, D. W.; Mark, J. E.; McCarthy, D.; Jian. L.; Sun, C.-C.; Farago, B. *Mater. Res. Soc. Symp. Proc.* **1990**, *171*, 57.
(12) Wilkes, G. L.; Orler, B.; Huang, H. H. *Polym. Prepr. (Am. Chem. Soc., Div. Polym. Chem.)* **1985**, *26* (2), 300.
(13) Huang, H. H.; Orler, B.; Wilkes, G. L. *Macromolecules* **1987**, *20* (6), 1322.
(14) Noell, J. L. W.; Wilkes, G. L.; Mohanty, D. K.; McGrath, J. E. *J. Appl. Polym. Sci.* **1990**, *40*, 1 177.
(15) Wang, B.; Wilkes, G. L. *J. Polym. Sci., Part A: Polym. Chem.* **1991**, *29*, 905.
(16) Brennan, A. B.; Rodrigues, D. E.; Wang, B.; Wilkes, G. L. *J. Inorg. Organomet. Polym.* **1991**, *1*, 167.
(17) Wang, B.; Brennan, A. B.; Huang, H. H.; Wilkes, G. L. *J. Macromol. Sci. Chem.* **1990**, *A27* (12), 1449.
(18) Wilkes, G. L.; Brennan, A. B.; Huang, H. H.; Rodrigues, D. E.; Wang, B. *Mater. Res. Soc. Symp. Proc.* **1990**, *171*, 15.
(19) Brennan, A. B.; Wilkes, G. L. *Polymer* **1991**, *32*, 733.
(20) Rodrigues, D. E.; Brennan, A. B.; Wang, B.; Betrabet, C. B.; Wilkes, G. L. *J. Mater. Chem.* **1992**, *4*, 1437.
(21) Rodrigues, D. E.; Wilkes, G. L. *J. Inorg. Organomet. Chem.* **1993**, *3*, 197.
(22) Landry, C. J. T.; Coltrain, B. K.; Brady B. K. *Polymer* **1992**, *33*, 1486.
(23) Landry, C. J. T.; Coltrain, B. K.; Wesson, J. A.; Zumbulyadis, N.; Lippert, J. L. *Polymer* **1992**, *33*, 1496.
(24) Landry, M. R.; Coltrain, B. K.; Landry, C. J. T.; O'Reilly, J. M. *J. of Polym. Sci.: Part B: Polym. Phys.* **1955**, *33*, 637.

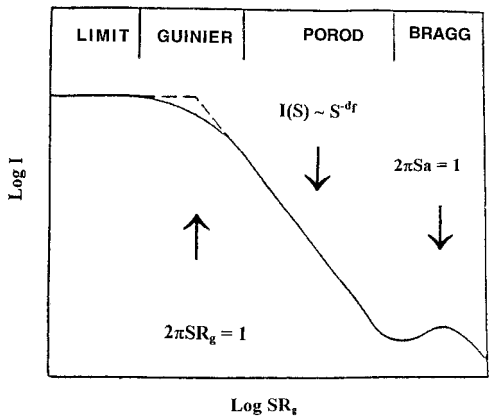

Figure 1. Schematic small-angle X-ray scattering curve when plotted on log I vs log sR_g scales.[3]

of these developments it was decided to attempt a study of the growth and development of these silicate particles using small-angle X-ray scattering and to analyze the results in terms of fractal dimensions. Transmission electron microscopy (TEM) was used to study the phase separation as well as the fractal structures of these particles present in the system. This study will then focus on the growth and structure of the particles developed in the PMMA matrix as a function of (a) metal alkoxide content and (b) temperature.

Structure from Small-Angle X-ray Scattering. As mentioned above, the structure of the silicate particles can often be discussed in the terms of their fractal dimensions. Fractals are of two types: mass and surface. Mass fractals are those where, in addition to dilational symmetry, the mass M of the particulate increases less rapidly than the volume it occupies[25] and hence $M \sim L^D$, where L is the characteristic particle size and D is the fractal dimension whose value will be less than the dimensionality of the particle. Surface fractals, on the other hand, are compact structures with a rough outer surface. The surface fractal dimension is a measure of surface roughness and is typically expressed as $S \sim L^{(D_s)}$ where S is the surface area and D_s is the surface fractal dimension. The fractal dimensions (mass or surface) can be obtained from the slope x of the scattering curve in the Porod region.[26] For mass fractals, the Porod slope $x = -D$, while for surface fractals $x = D_s - 6$. For slit-smeared data where an infinite slit approximation can be assumed, the Porod slope lies between O and -2 for mass fractals, while for surface fractals it lies between -2 and -3. Slit-smeared data (which is how all the data in this paper was obtained) can be adjusted to that obtained from pinhole collimation by adding a factor of -1 to the measured Porod slope. This was our procedure used in this report. Again, it should be noted that this factor can be added on only if the dimensions of the slit are such that it can be considered of infinite length.[25,26]

Average radius of gyration $<R_g>$ measurements were made in the Guinier regime of the scattering profiles as shown in Figure 1. Guinier[27] showed that, for a dilute monodisperse particulate system, in which the particles assume all orientations with equal probability, the scattered intensity can be described by a series expansion as follows:

$$I(\mathbf{s}) = I(0)\{1 - 4\pi^2 (\mathbf{s}^2 \langle R_g^2 \rangle)/3 \ldots\}^1$$

The function $I(0)$ is the scattered intensity at zero angle, which is proportional to the total number of irradiated electrons in the system, and $<R_g^2>$ is the electronic squared radius of gyration. The term **s** is the scattering vector and is equal to $(2/\lambda)\sin\theta$ where λ is the wavelength of the incident radiation and θ is one-half of the radial scattering angle.

Experimental Section

Five grams of PMMA of molecular weight $M_n = 67\,000$ g/mol were first dissolved in 20 mL of tetrahydrofuran (THF). The mixture was stirred at 45 °C until all the polymer was completely dissolved. In a separate flask containing 5 g of THF, water was added to TEOS in a stoichiometric amount of 100 wt % necessary to theoretically hydrolyze all the alkoxy functionalities present in the reaction mixture. To this water−TEOS−THF mixture was added the acid catalyst (10 N HCl) in a stoichiometric amount of 0.048 (mol/mol) of the alkoxy functionalities. The clear water−TEOS−THF−acid mixture was added to the THF−PMMA mixture after 10 h. The time period of 10 h was chosen arbitrarily to allow some of the TEOS to hydrolyze to form silanol moieties. The water−TEOS−THF−acid mixture remained clear indicating no macrophase separation. The reactants were stirred for 24 h at room temperature and then cast into Teflon Petri dishes, where they developed into films at room temperature. The films usually were well formed 10 to 12 h after casting. Films produced utilizing the above reactants are denoted as TEOS(X)−PMMA-100−0.048 where X is the weight fraction of TEOS to PMMA expressed as a percent of initial reactants. During the preparation of *some of the films*, a small amount of DMF (0.1 mL) was added to the solution of PMMA and THF[1] as soon as the PMMA was dissolved. This was done in view of the fact that some previous work conducted by the authors and their co-workers[18−21] indicated that DMF tends to change the structure of the resulting silicate particles significantly.[3] These specific films will be denoted as TEOS(X)−PMMA-100-0.048−0.1 mL of DMF. Following film preparation, all films were then annealed at 140 °C for periods of 5 min, 30 min, or 5 h in a forced air convection oven preset to the required temperature. Similar to the procedure described in ref 5, the films were then removed and immediately quenched in liquid nitrogen to stop any further reaction or diffusion. SAXS and TEM was then performed on all these films, including films cast at room temperature that had not been subjected to annealing.

SAXS data was obtained on a Siemens-Kratky camera system with a M. Braun position sensitive detector from Innovative Technology, Inc. The Cu Kα (wavelength = 1.54 Å) X-rays were generated with a Philips Model 1792 generator operated at 40 kV and a beam current of 20 mA. A Nickel filter was used to minimize the intensity of Cu Kβ radiation. All data were obtained using an "infinite" entrance slit of width 100 μm. A standard Lupolen (polyethylene) sample was employed to measure the X-ray intensity of the primary beam. A lead stearate sample with a discrete small angle d spacing of 49.5 Å was used to calibrate the detector on a daily basis. For every sample, the scattering intensity was measured at the sample and parasitic position. The latter was subtracted from the former to obtain the sample scattering profile. TEOS−PMMA samples used for scattering had a thickness of 5−10 mil, which was several times greater than the $<R_g^2>^{1/2}$ of the scattering particles. All the scattering data presented in this paper were smoothed using an ASYST routine developed in our laboratory. A smoothed profile superimposed on the regular profile is shown in Figure 2. for the TEOS[40]−PMMA-100−0.048 specimen heated to 140 °C for 5 h. As can be seen in this plot there is no significant change in the profile before and after smoothing. Further, the radius of gyration

(25) Keefer, K. D. *Mater. Res. Soc. Symp. Proc.* **1986**, *21*, 295.
(26) Schaefer, D. W.; Keefer, K. D. *Phys. Rev. Lett.* **1984**, *53*, 1383.
(27) Guinier, *A. Ann. Phys.* **1939**, *12*, 161.

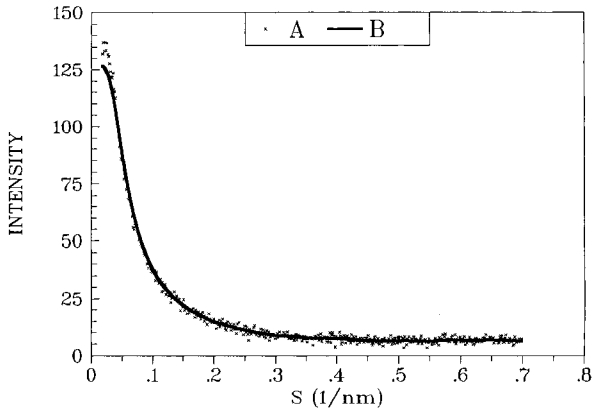

Figure 2. Curve A is that of the actual SAXS data collected, while curve B represents the smoothed value.

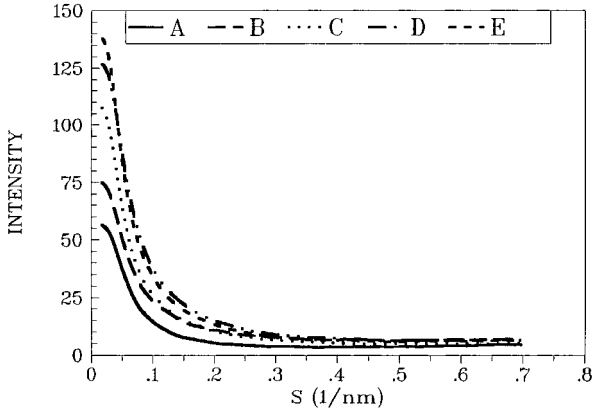

Figure 3. Plot of scattered intensity for the materials TEOS(X)−PMMA-100−0.048 reacted in THF and annealed to 140 °C for 5 h, where X is the weight percent of TEOS represented by curve A at 10%, B at 20%, C at 30%, D at 40%, and E at 50%.

and the Porod slope were found to be the same before and after smoothing substantiating our claim above.

TEM was performed on a Philips 420 microscope. The samples were first microtomed at room temperature using a Reichert-Jung microtome with a diamond knife. The microtomed sections typically have a thickness of 500 − l000 Å. TEM was performed utilizing a operating voltage of l00 kV.

Results and Discussion

Effect of TEOS Weight Fraction on the Films Reacted in THF. The scattering profiles for the TEOS−PMMA films reacted in THF and treated to 140 °C for a period of 5 h are shown in Figure 3. These profiles do not reveal a maxima or interference peak in the SAXS profile and differ from many of the previous systems investigated such as TEOS−PTMO (18−20) or TEOS−PEK[14] where microphase separation occurs and displays a spatial periodicity that is dependent upon the molecular weight of the end functionalized organic species and the concentration of the reactants. The profiles suggest an increase in the scattering intensity at zero angle $I(0)$ with an increase in the weight percent of TEOS from 10% to 50%. When the SAXS data shown in Figure 3 is analyzed in the Guinier and Porod regimes, it is found that there is very little variation in the radius of gyration or the fractal dimensions as the TEOS weight percent is increased from 10% to 50%. The average root-mean-square radius of gyration as measured from the Guinier region varies from 43 to 50 Å as

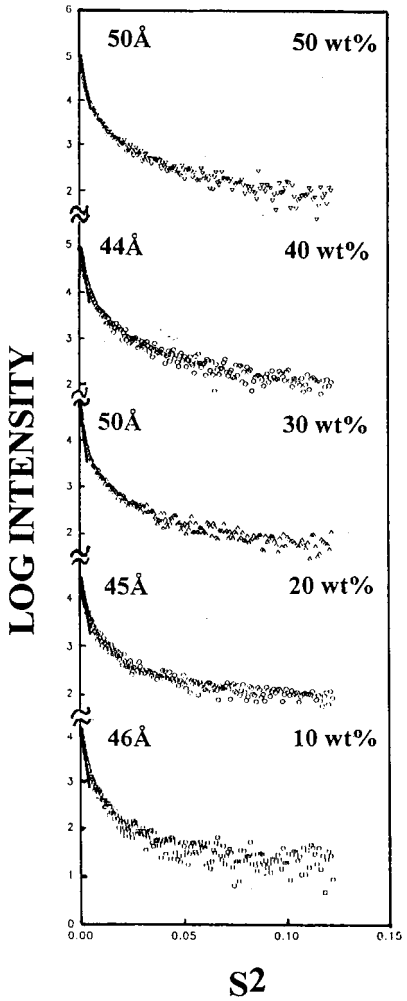

Figure 4. Guinier Plot for the system TEOS−PMMA system reacted in THF. The numbers in the figure indicate the weight percent TEOS as well as the values of $<R_g^2>^{1/2}$.

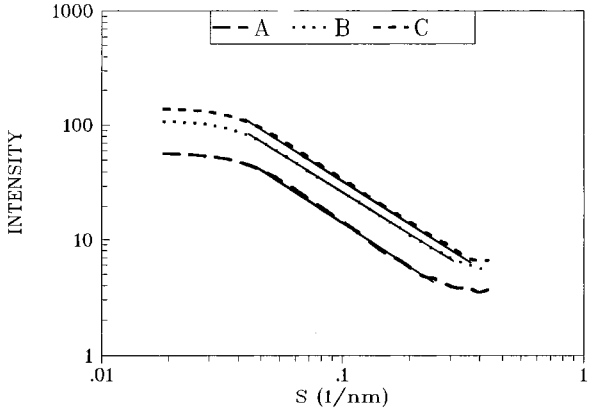

Figure 5. Porod plot for the materials TEOS(X)−PMMA-100−0.048 reacted in THF and annealed to 140 °C for 5 h, where X is the weight percent of TEOS represented by A at 10%, B at 30%, and C at 50%.

can be seen from the Guinier plots shown in Figure 4. In Figure 5, the Porod plots are shown for the materials containing 10, 30, and 50 wt % TEOS and it can be seen that there is little variation in the respective slopes as the metal alkoxide content is increased. Table 1 shows the fractal dimension as well as the radius of gyration of the silicate particles as the weight fraction of TEOS is increased. The Porod slope is approximately −2.4, indicating that the particles are mass fractals. These

Table 1. Values of Radius of Gyration $[R_g^2]^{1/2}$ and the Fractal Dimension (D) for the TEOS(X)−PMMA100-0.048 Films Reacted in THF and Annealed at 140 °C for 5 h

TEOS content (wt%)	radius of gyration $\langle R_g^{1/2})^2$ (Å)	fractal dimension (D)
10	46	2.44
20	45	2.42
30	50	2.36
40	44	2.37
50	50	2.42

particles are believed to be formed by a nucleation and growth process involving diffusion limited growth. In this type of growth process, monomer molecules take Brownian trajectories during the process of phase separation and subsequently diffuse toward a silicate cluster. Witten and Sander[28] have shown that in this growth process the monomer sticks with the cluster on first contact and hence growth in these systems occurs mostly at the exterior positions or on outer sites of the growing cluster and results in a fractal dimension of 2.45. These results, when taken in conjunction with the increasing scattering intensity as weight fraction increases, suggest that there must be a larger number of such microscopic scattering particles as the TEOS weight fraction is increased—recall Figure 2. Interestingly, the data also suggests that, for the range of PMMA weight fraction utilized, it has no effect on the size or structure of the microscopic particles formed.

TEM results for these TEOS−PMMA materials are shown in Figure 6. The 10 wt % film as seen in Figure 6a does not provide resolution of any silicate particles, possibly because there is a low density of particles in the PMMA matrix. The silicate particles are the dark phases in these micrographs because of their higher electron density when compared with those of the PMMA. At 20 wt % TEOS, some small particles are visible as compared with the 10 wt % film; however, these features are not well resolved. These silicate particles are more open and wispy as compared with those reacted in the cosolvent system of THF and DMF, which will be discussed later. In the micrographs displayed in Figure 6 for the 20 wt % TEOS−PMMA material, another larger oval shaped feature can be seen indicating that these materials display two levels of structure. While these larger silicate particles can be seen in all materials containing 20 wt % TEOS and above, *they cannot be seen in the micrographs 6c−e since these were imaged in regions containing no large particles*. These larger particles are typically 0.2−0.5 mm in size. Landry and co-workers[22] have previously documented that these larger silicate particles appear to form early in the phase separation process and their size appears to be dependent upon the film thickness. It appears that their size and density is dependent upon the TEOS content as well. The formation of these particles potentially could be investigated using light scattering. However, the authors have not been able to perform these experiments at the present time. The transparency of the TEOS−PMMA films is not significantly decreased by the occurrence of these larger silicate particles because they are not present in large numbers until the TEOS content is raised to 60 wt %. These distinct particles will be discussed in further detail later in this paper. As the TEOS content is increased further, larger numbers of these sub-microscopic silicate particles can be seen in the photomicrographs in Figure 6c, d, and e which represents the 30, 40, and 50 wt % TEOS−PMMA samples, respectively. This increase in the number of scattering particles seen in the micrographs correlates very well with the increase in the scattering intensity at zero angle $I(0)$ which is in turn directly proportional to the number of "excess" electrons in the irradiated system.

As the TEOS weight fraction is increased to 60%, the films become hazy indicating that the phase-separated silicate particles are large enough to scatter light. These films were annealed at 140 °C in an attempt to determine whether any additional microphase separation would take place. The SAXS plot shown in Figure 7 does not show any major change in scattering intensity as compared with that in the films containing lower weight fractions of TEOS, even when the film is annealed at 140 °C for 5 h. This slight change in scattering intensity may be due to densification of the silicate particles at 140 °C promoted by some furthering of the sol−gel reactions. The much lower intensity of this 60% TEOS system is because most of the silicate particles are now outside the size regime of small-angle X-ray scattering. These results indicate that there exists a critical point at an initial TEOS weight percent between 50 and 60 at which a complete transition from microphase to only macrophase separation occurs. The TEM photomicrograph shown in Figure 8 reveals the macroscopic domains in the 60 wt % TEOS−PMMA system. These domains are elongated in a direction parallel to the casting substrate and the striations marked across them are believed to be distinctly caused by stress marks formed during the microtoming of the films. When microtomed in a direction *parallel to the surface* of the substrate, the cross section of these large silicate particles is circular as can be seen in Figure 9. These micrographs show that the *small* silicate particles having fractal dimensions of 2.4 seen in the TEOS−PMMA films containing 10−50 wt % are *no longer present* in the 60 wt % material, thereby supporting the earlier SAXS data and general analysis.

As stated above, Landry and co-workers[22,23] also found these large silicate particles in their TEOS−PMMA films and showed these particles to be disk shaped. The size of the particles and their numbers increased from top to bottom of the film. The authors of this paper support their results. As stated by Landry et al., the development of these larger silicate particles is a kinetic process and their presence is dependent upon film thickness. They proposed that, under acidic conditions, the TEOS polymerized to form ramified nonhardened structures; these ramified structures existed in the form of somewhat soft spheres which eventually were deformed to form disks during the drying process. The increase in the size of these larger silicate particles from top to bottom was attributed to the more rapid evaporation of solvent from the upper or air surface of the film as compared with the lower or substrate surface. This caused the upper surface of the film to vitrify first while in the lower portions a large solvent concentration allowed the silicate "chains" more mobility which permitted them to grow to form larger particles. Our observation of only macrophases in the TEOS−PMMA material containing 60 wt % TEOS suggests that the

(28) Witten, T. A.; Sander, L. M. *Phys. Rev. Lett.* **1981**, *47*, 1400.

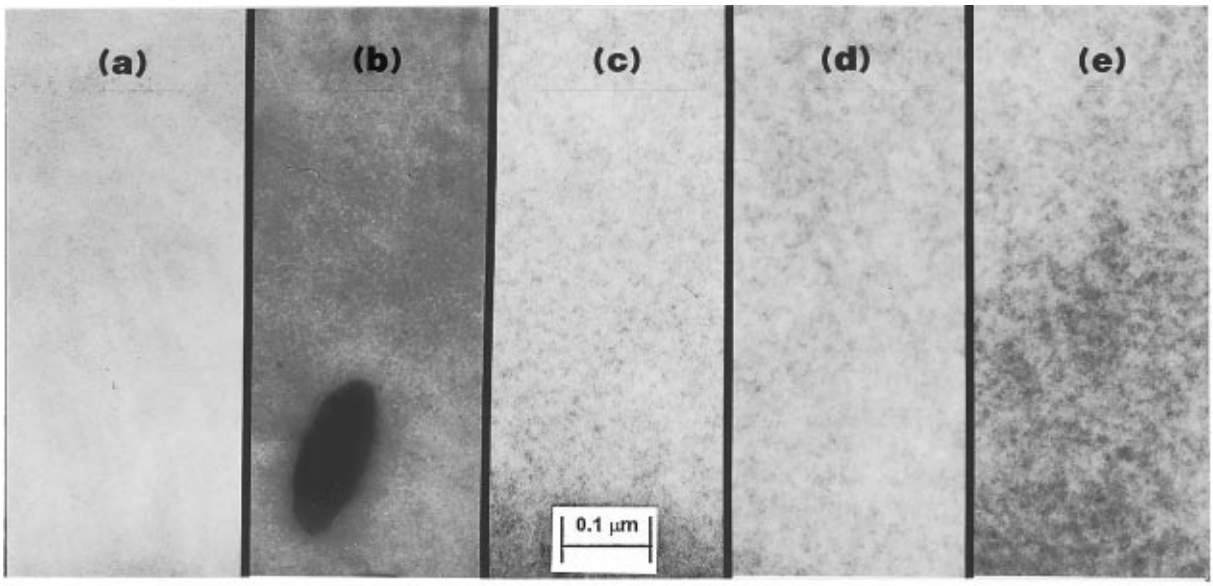

Figure 6. TEM micrographs of the TEOS(X)−PMMA-100−0.048 system reacted in THF and annealed to 140 °C for 5 h. X is represented by curve *a* at 10 wt %, *b* at 20 wt %, *c* at 30 wt %, *d* at 40 wt %, and *e* at 50 wt %.

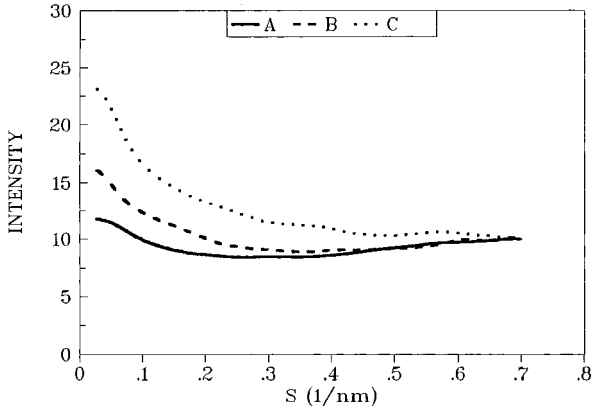

Figure 7. Small-angle X-ray scattering profile for the system TEOS^{60}−PMMA-100−0.048, where the profile A is for the room-temperature-annealed film and B and C are the profiles for the materials annealed to 140 °C for 30 min and 5 h, respectively.

development of such phases in the materials containing less than 50 wt % TEOS initially may also be partially due to the concentration fluctuations in the lower portions of the film where the weight fraction of TEOS to PMMA is greater than or equal to 0.6. This observation is further supported by the fact that in the 10 wt % TEOS−PTMO system there is no macrophase separation of any kind as seen from TEM, indicating that in this system there is never enough silicate to ever promote agglomeration and formation of the larger structures. Landry and co-workers have also reported that, in the acid-catalyzed systems, there occurs hydrogen bonding between the polymeric silica and the PMMA chains. These hydrogen-bonding interactions prevent the two components from completely macrophase separating. It could be *speculated*, that when the volume fraction of silicate chains (SiO_2) at a localized region in the PMMA is such that the intramolecular interactions between the silicate chains exceeds the number of intermolecular interactions between the silicate and the PMMA, then such macrophase separation occurs in the system. In other words (since the silicate and the PMMA are incompatible with each other) as the size of the silicate particle grows larger, its surface area decreases, which consequently reduces the number of possible hydrogen bonding interactions between the hydroxyl moieties of the silanol and the PMMA, which causes the macroscopic phase separation.

Effect of TEOS Weight Fraction on the Films Reacted in THF and 0.1 mL DMF. With the addition of 0.1 mL of DMF, the features of the scattering particles greatly change as can be seen from Table 2, in which the fractal dimension and the radius of gyration for the materials containing 10−30 wt % TEOS are displayed. From this table it can be seen that the fractal dimension for the 10 wt % TEOS−PMMA material is now 3.0 and the radius of gyration is 59 Å. Both, the radius of gyration and fractal dimension for the system reacted in THF−DMF are distinctly greater than those for the silicate particles produced by the reaction in THF. The fractal dimension in this case indicates that the silicate particles are now surface fractals rather than mass fractals. DMF has a pH of 6.7 (0.5 M solution in water) and from previous work it has been found that it causes the silicate phase to undergo a more pronounced separation from the organic as well as to be more particulate like.[20,21] Surface fractals are typically produced by reaction limited monomer cluster aggregation wherein there is a barrier to reduce the "probability of permanent attachment" (condensation rate), so that many collisions are required between monomer and cluster to form a bond. Since all possible reaction sites are therefore accessed with equal probability, this mode of reaction would lead to smooth clusters with fractal dimension = 3. This mode of aggregation is appropriately called reaction limited cluster aggregation. Under basic conditions it has been reported by Iler[29] that silica has a highly negative surface charge which promotes the barrier mentioned above and that the resulting electrostatic repulsion suppresses particle aggregation. Brinker and co-workers[30,31] have also reported that under basic conditions the silicate particles tend to be

(29) Iler, R. K. *The Chemistry of Silica* Wiley: New York, 1979.
(30) Brinker, C. J.; Keefer, K. D.; Schaefer, D. W.; Ashley, C. S. *J. Non-Cryst. Solids* **1982**, *48*, 47.

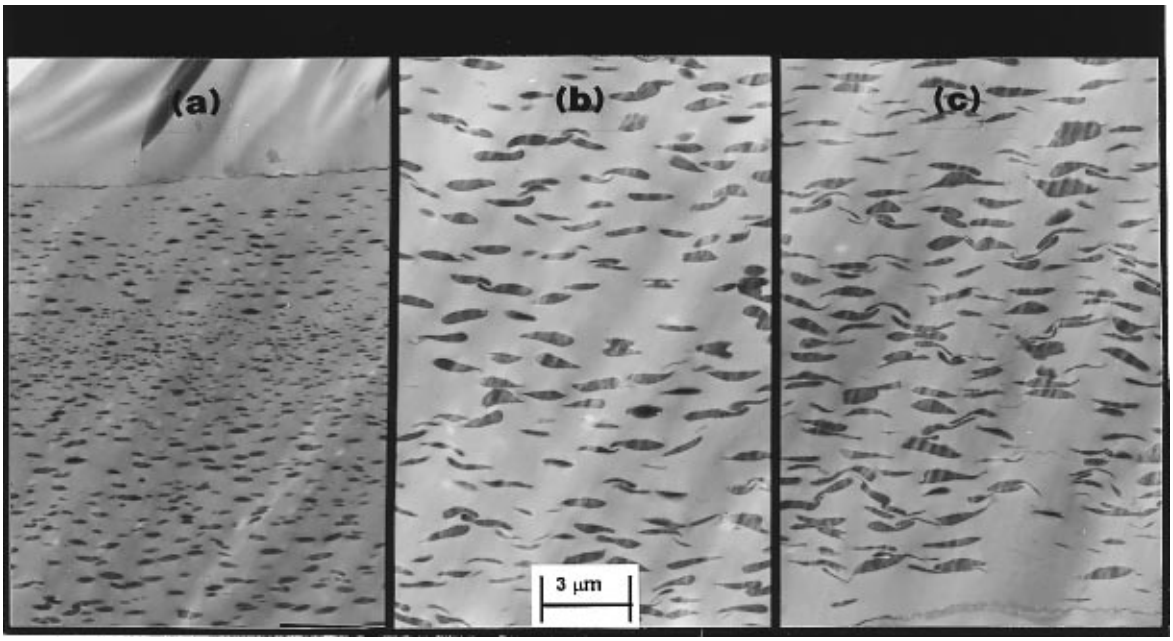

Figure 8. TEM micrograph of the TEOS^{60}−PMMA-100−0.048 system reacted in THF shows the macroscopic particles across top, middle, and bottom sections of a film. The top and bottom sections of the film show epoxy in which the film was embedded before microtoming.

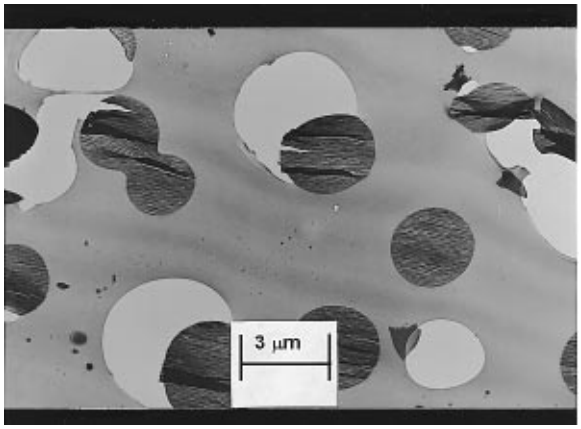

Figure 9. TEM micrograph shows sectional view parallel to the casting substrate of the TEOS^{60}−PMMA-100−0.048 system reacted in THF.

Table 2. Radius of Gyration and Fractal Dimension for TEOS−PMMA Reacted in THF and 0.1 ML of DMF

TEOS content (wt%)	radius of gyration $[R_g^{1/2}]^2$ (Å)	fractal dimension (D)
10	59	3.00
20	63	2.90
30	50	2.45

more convoluted than under acidic conditions. DMF has also been reported to hydrogen bond with the hydroxyl moiety of silanol[4,5] and this bonding may serve to suppress particle aggregation. Thus particle formation in this TEOS−PMMA system appears to proceed by a monomer−cluster growth process, which produces more compact, surface-roughened convoluted particles.

As the TEOS composition is increased to 20% and 30 wt %, in the DMF containing systems the microscopic silicate particles are found to be less convoluted. At 20 wt % the fractal dimension is reduced to 2.9, while at 30 wt % the fractal dimension is reduced to 2.45. Both of these dimensions clearly suggest mass fractal development. The average radius of gyration for the 20 wt % material is 63 Å, while it is decreased for the 30 wt % material to 50 Å. This gradual decrease in the fractal dimension with increasing initial TEOS content is, however, accompanied by an increase in the number of macroscopic silicate particles as seen in the TEM micrographs in Figure 10. In these micrographs it can be seen that, as the TEOS content is increased from 10 to 40 wt %, the number of particles increases. In Figure l0a, even for the 10 wt % TEOS−PMMA film, it can be seen that there are discrete silicate particles visible. In Figure l0b, (representing the 20 wt % system) these particles can be seen to increase in number, while in Figure l0c,d (representing the 30 and 40 wt % systems, respectively) there are more and more silicate particles visible, but these are more ramified as compared with those seen in Figure l0a,b. This decrease in the fractal dimensions with increasing TEOS content may possibly be attributed to the limited amount of DMF added to these reactions. As the TEOS content increases, the DMF molecules present in the reaction mixture will likely not be able to hydrogen bond with all the hydroxyl moieties, thereby causing the growth to be a combination of reaction limited monomer−cluster and diffusion-limited monomer−cluster, which causes a reduction in the overall fractal dimension. It is expected that the monomer−cluster growth will possibly precede the cluster−cluster growth, since the condensation rate in the base-catalyzed systems is known to be more rapid than hydrolysis. As the number of DMF hydrogen bonded SiOH moieties decreases, the tendency toward either diffusion-limited monomer−cluster growth or cluster−cluster growth will increase. Thus, as TEOS content increases, there is a consequent decrease in the fractal dimension.

Another factor to be considered in the growth of the microscopic silicate particles is the equilibrium between the larger (macroscopic) particles and the TEOS monomer itself. As the weight fraction of TEOS is increased

(31) Brinker, C. J.; Keefer, K. D.; Schaefer, D. W.; Assink, R. A.; Day, B. D.; Ashley, C. S. *J. Non-Cryst. Solids* **1984**, *63*, 45.

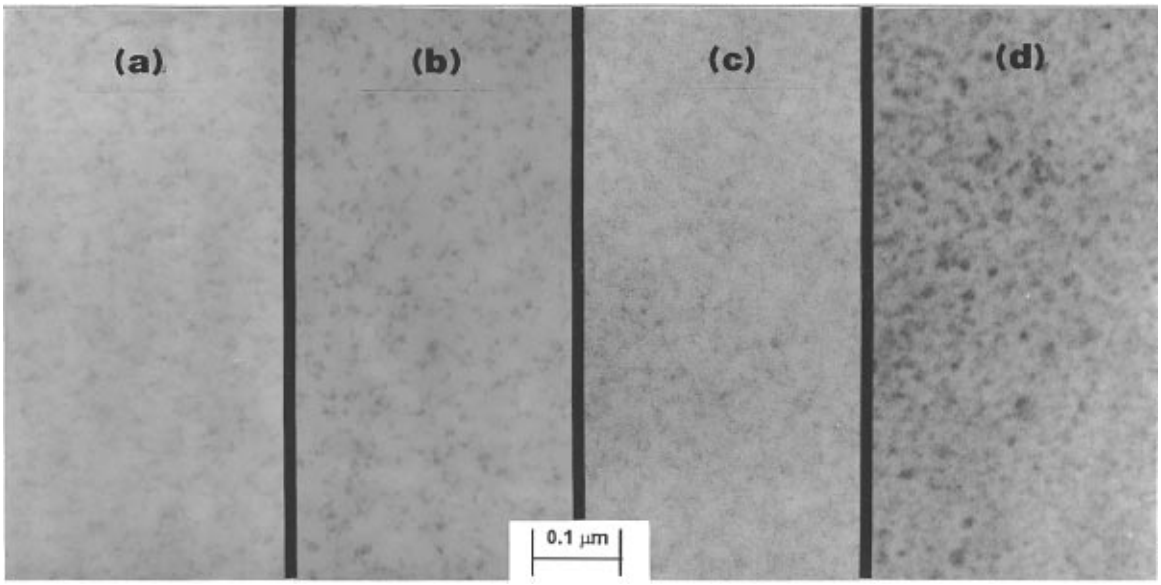

Figure 10. TEM micrograph of the TEOS(*X*)−PMMA-100−0.048 material reacted in THF−0.l mL of DMF and annealed to 140 °C for 5 h. *X* is represented by part a at 10 wt %, b at 20 wt %, c at 30 wt %, and d at 40 wt %.

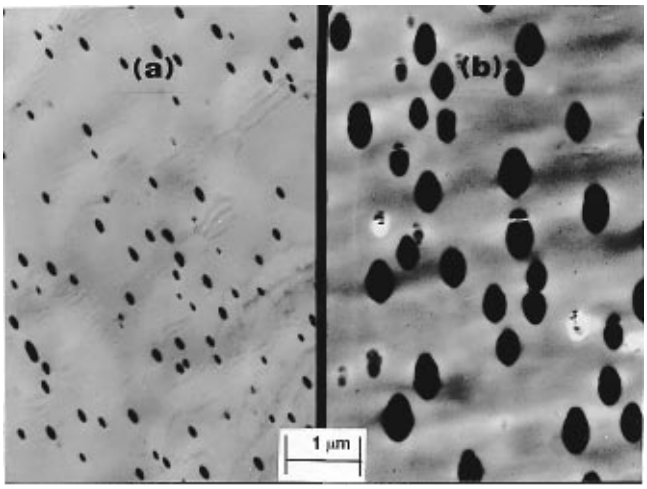

Figure 11. TEM micrograph of the TEOS[20]-PMMA-100−0.048 system reacted in (part a) THF and (part b) THF−0.l mL of DMF showing the difference in sizes between the macroscopic silicate particles.

in these systems (where DMF is used in conjunction with THF as a cosolvent), the number of macroscopic particles (large silicate particles with sizes ranging from 0.2 to 0.5 mm) increases. The growth of these larger particles appears to be facilitated by the presence of DMF. The DMF may possibly cause the development of a large number of nucleation sites for these macroscopic particles. These macroscopic particles are in general larger in size than their counterparts grown only in THF as can be seen in Figure 11 which shows sections of the film containing 20 wt % TEOS−PMMA reacted in only THF or in a mixture of THF−0.l mL of DMF. As the macroscopic SiO_2 particles increase in size, there is less TEOS left to polymerize into the micro-silicate particles. If this speculation is correct, this would prevent the growth of these microscopic particles into highly condensed structures since it would be difficult for a grown cluster to easily migrate in the polymeric matrix of PMMA. Since monomer−cluster growth is believed to occur first in the systems containing DMF, a larger number of clusters are formed early during the casting process. With the passage of annealing time at 140 °C, these micro-silicate clusters grow in size due to depletion of the surrounding monomer from the matrix. In the systems reacted in THF−0.l mL of DMF, once the micro-silicate clusters have been formed initially, the lack of much hydrolyzed monomer being hydrogen bonded to DMF would require a change in the growth mechanism, thereby requiring cluster−cluster growth. Since it is difficult for a micro-silicate particle to migrate through the PMMA matrix, the result is a larger number of smaller particles being of a lower fractal dimension. It is the authors intention that these are competing kinetic pathways when a small amount of DMF is added to the reaction mixture. There is competition to form the microscopic surface fractal clusters versus the large macroscopic particles. Once this initial structure is set in the PMMA matrix, additions to the microscopic particles, as a result of annealing, are believed to occur by a diffusion-limited mechanism, which changes the fractal structure to more of a mass fractal.

Effect of Annealing at 140 °C on the TEOS−PMMA Films. *(a) Reaction in THF.* As stated earlier, one of the purposes of this work was to study the growth of the sub-microscopic silicate particles in the PMMA matrix. The next portion of this paper will deal briefly with the growth of these particles when the films were annealed at 140 °C. To study this growth behavior, SAXS and TEM were performed on the 40 wt % TEOS−PMMA film as a function of annealing time at 140 °C. As stated earlier, a given film was annealed at 140 °C for periods of 5 min, 30 min, and 5 h. It should be pointed out that this annealing temperature is well above the glass transition temperature of PMMA, which is ca. 105 °C, and hence diffusion of the smaller silicate species can still take place to facilitate nucleation and growth. Here the samples were annealed in a forced air convection oven preset at 140 °C. The samples were removed after either 5 min, 30 min, and 5 h and quenched in liquid nitrogen to prevent any further reaction. Following this they were subjected to SAXS. The SAXS profiles are displayed in Figure 12. In this figure it can be seen that the scattering intensity increases significantly with annealing time and this

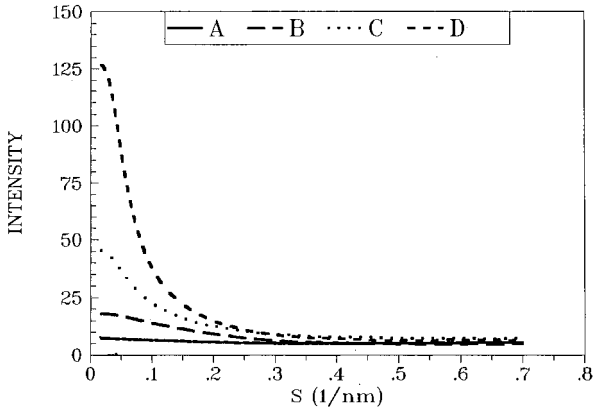

Figure 12. Scattering intensity for the TEOS[40]−PMMA-100−0.048 system reacted in THF, where curve A represents room-temperature-annealed material, B at 140 °C at 5 min, C at 140 °C at 30 min, and D at 140 °C at 5 h.

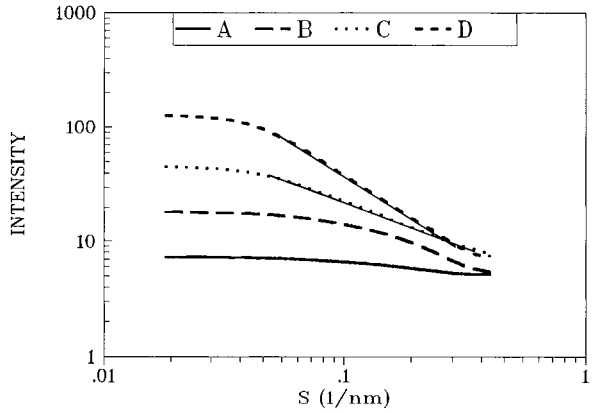

Figure 13. Porod plot for the TEOS[40]−PMMA-100−0.048 system reacted in THF, where curve A represents room-temperature-annealed material, B at 140 °C at 5 min, C at 140 °C at 30 min, D at 140 °C at 5 h.

may be related to an increase in the number of scattering particles as well as due to an increase in the electron density of the silicate phase as the level of condensation increases. When these results are plotted on a log−log scale, as in Figure 13, it can be seen that there is an increase in the fractal dimension with annealing time at 140 °C. The scattering profiles obtained on the room temperature and 5 min (140 °C) cured films do not contain linear regions in the Porod regime where fractal dimensions can be obtained. When retained at 140 °C for 30 min, the fractal dimension is 1.8, while after 5 h the fractal dimension is 2.4. At the same time it was found that the radius of gyration was increased from 9 Å for the room-temperature cured film, to 43 Å for the film heated to 140 °C for 5 h, as can be seen in Figure 14. Since these particles are expected to grow by a monomer−cluster growth mechanism where the diffusing reactive species react on first contact, the increase in the convolutedness with annealing time is believed to be due to reorganization within the silicate particles. The TEM's for this set of materials is shown in Figure 15. Figure l5a shows no particulates for the room-temperature-cured material because this is below the resolution of the microscope. A few small particulates can be seen in the micrograph Figure 15b of the material heated to 140 °C for 5 min. The particulates are larger in size as well as in number for the material heated for 30 min[15c] while in the material heated for 5 h the particulates are the largest

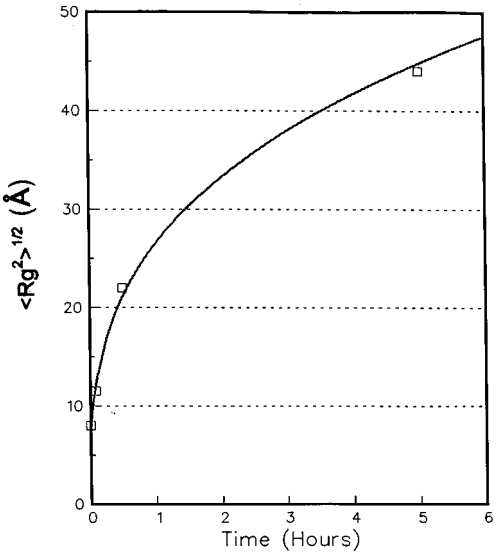

Figure 14. Plot illustrates the sub-microscopic particle growth as measure from the SAXS profiles for the TEOS[40]−PMMA-100−0.048 system reacted in THF.

(Figure l5d) thus corresponding with the data obtained from SAXS. These results indicate that there is no single nucleation event occurring in these materials and that nucleation and growth occurs throughout the reaction period. With the increase in time at 140 °C, there is a diffusion process occurring in these materials during which the particle nucleates and consequently grows in size. The nonuniform nucleation followed by the diffusion of monomer to the nucleation sites allows for a broad distribution in particle size as can be seen in the micrograph in Figure 15d.

(b) Reaction in THF and 0.1 mL of DMF. The films containing an initial TEOS content of 20 wt % and reacted in THF−0.l mL of DMF were also subjected to annealing at 140 °C for periods of 5 min, 30 min, and 5 h. The SAXS results are shown in Figure 16 where again it can be seen that there is an increase in the scattering intensity with time at 140 °C. When the scattering profiles of Figure 16 are plotted on a log−log plot as in Figure 17 it can be seen that the fractal dimension of the particle increases with annealing time. At 5 min, the Porod slope provides a fractal dimension of 2.15 which increases to 2.83 after 30 min. After 5 h the fractal dimension is 2.91, which indicates a highly convoluted mass fractal structure. The linear slopes in the scattering data presented in Figure 17 are less than one decade in size and hence the fractal dimensions are at best only an approximation. However, it is important to note that these scattering curves are *quite different* than those curves obtained for samples with no DMF! The particle growth is believed to be due to reaction limited monomer−cluster interactions, and therefore the increasing fractal dimension is more likely to be a result of multiple collisions between monomer and cluster rather than internal rearrangement within the cluster as in the previous case. Since a large number of sites are accessed by the monomer, there are better opportunities for extensive condensation resulting in a more convoluted particle. The increase in the radius of gyration with time for these particles is shown in Figure 18. These particles are significantly larger than those grown in THF. The basic nature of the DMF causes an increase in the condensation rate which

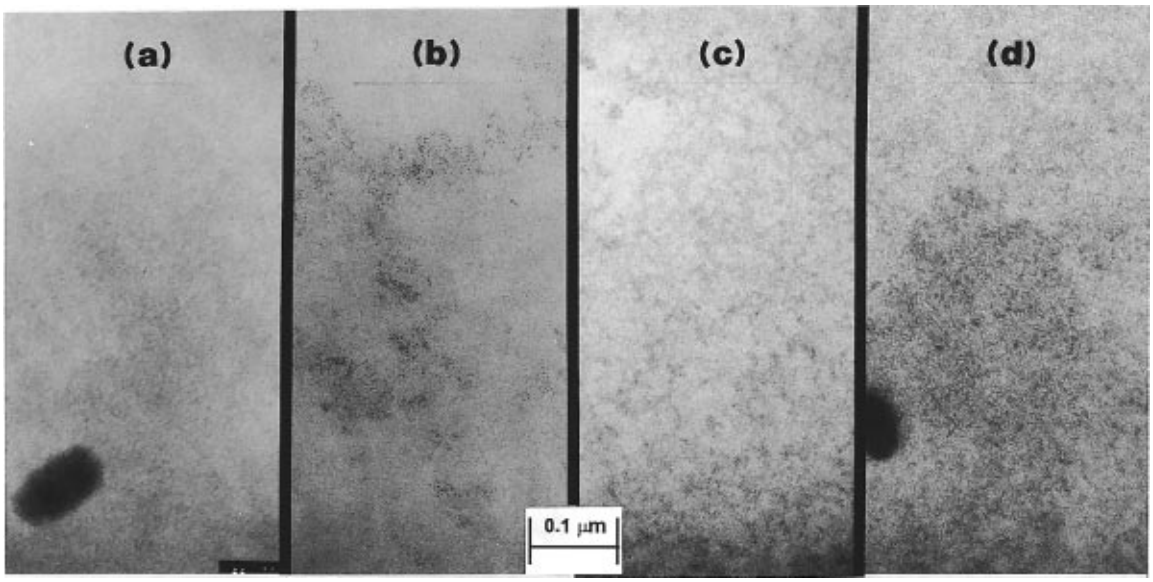

Figure 15. TEM micrograph of the TEOS[40]−PMMA-100−0.048 system reacted in THF. (Part a) displays a microtomed section annealed at RT, b at 140 °C at 5 min c at 140 °C at 30 min, and d at 140 °C at 5 h.

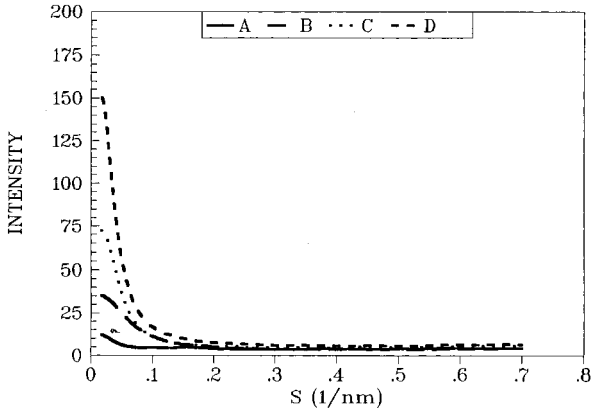

Figure 16. Scattering intensity for the TEOS[20]−PMMA-100−0.048 system reacted in THF−0.l mL of DMF, where curve A represents room-temperature-annealed material, B at 140 °C at 5 min, C at 140 °C at 30 min, and D at 140 °C at 5 h.

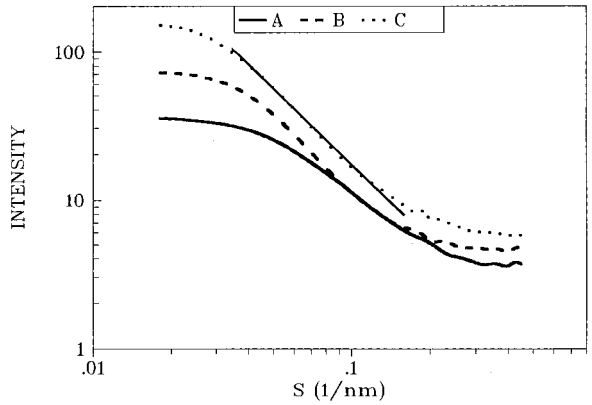

Figure 17. Porod plot for the TEOS[20]−PMMA-100−0.018 system reacted in THF−0.l mL of DMF, where curve A represents room-temperature-annealed material, B at 140 °C at 5 min, C at 140 °C at 30 min, and D at 140 °C at 5 h.

results in a larger particle size for these materials. Here the radius of gyration increases from 47 Å after 5 min of heating to approximately 63 Å after 5 h of heating. TEM micrographs for the 20 wt % TEOS−PMMA material are shown in Figure 19. Figure 19a−d represents the microstructure at room temperature, 5 min,

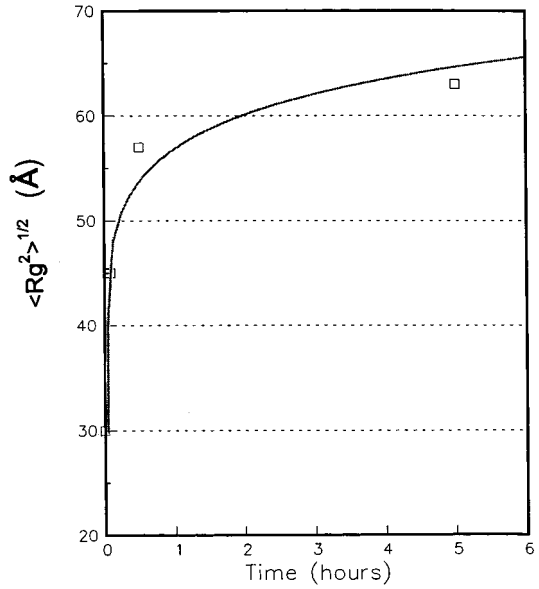

Figure 18. Plot illustrates the sub-microscopic particle growth as measured by $<R_g^2>^{1/2}$ from the SAXS profiles for the TEOS[20]−PMMA-100−0.048 system reacted in THF−0.l mL of DMF.

30 min, and 5 h at 140 °C. Figure 19a shows sub-microscopic particles even at room temperature, which is indicative of a rapid condensation rate. These particles are not highly resolved, which indicates that they are of a very small size. Also visible in this micrograph are the large macroscopic particles discussed earlier. These larger particles appear to have white halos around them. It is *speculated* that these halos are caused either by (a) the depletion of monomer (TEOS or its hydrolyzed form) during the casting process from the surrounding PMMA to form these macroscopic particles or (b) as a result of thickness variations (whiter regions indicating a thinner section of the film) in the vicinity of these particulates that resulted from the microtoming process. These macroscopic particles as seen in all the micrographs in Figure 18 have striations across them which are caused by the microtoming process. In Figure 19b, c, and d, which represent the morphology after 5 min, 30 min and 5 h

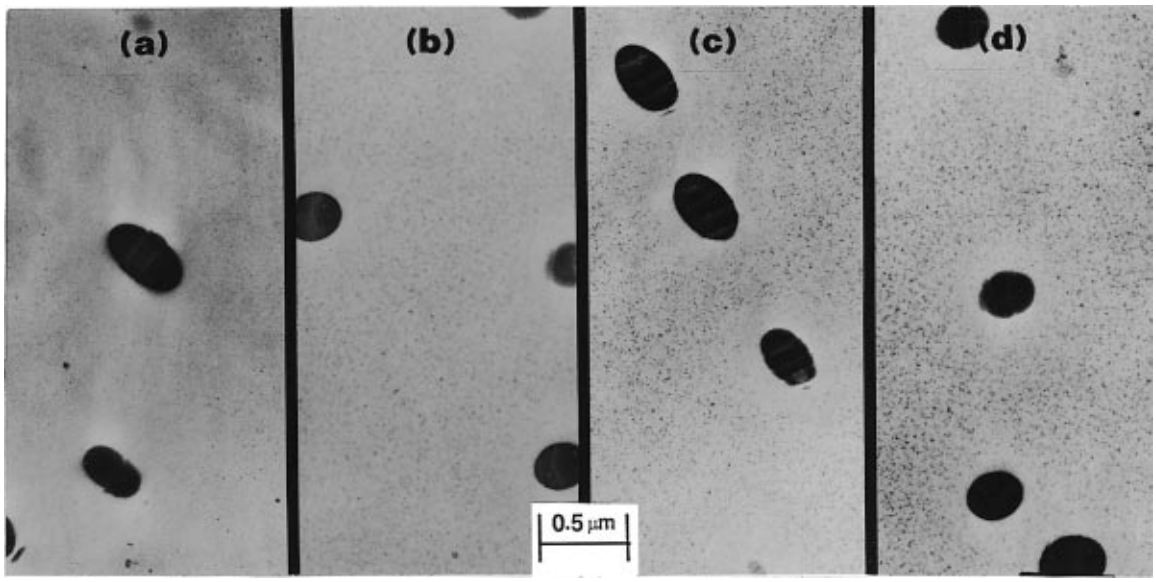

Figure 19. TEM micrograph of the TEOS[20]−PMMA-100−0.048 system reacted in THF−0.l mL of DMF. Part a displays a microtomed section annealed at RT, b at 140 °C at 5 min, c at 140 °C at 30 min, and d at 140 °C at 5 h.

at 140 °C, respectively, it can be seen that the sub-microscopic particles are larger with each increased interval of annealing time (as indicated by the SAXS results) and are consequently better resolved. It is difficult to determine whether there is an increase in the number of scattering particles from these micrographs. The presence of such sub-microscopic particles early in the casting process has an interesting ramification in that the structure of the particles is fixed very early during the casting process, especially when compared with the materials reacted in only THF where the structure is determined mostly by diffusion which occurs during annealing. However, the particles (reacted in THF−0.l mL of DMF) appear to be of different sizes which may possibly indicate that nucleation is not a spontaneous event or that there is a nonuniform growth rate for the particles in these materials.

Conclusions

This work has demonstrated that, when TEOS is reacted in the presence of PMMA and THF, the sub-microscopic particles display sizes which are independent of the TEOS content (up to 50 wt %) as are the fractal dimensions. These particles grow in size when annealed at 140 °C, and the nature of diffusion during the annealing process determines their structure. The PMMA content is found to have little effect on particle structure. Along with these sub-microscopic particles, large macroscopic disk-shaped particles are also formed whose growth is determined by kinetics and is therefore dependent upon the film thickness as well as the TEOS content. A drastic change in this phase separation behavior occurs when the initial weight fraction of TEOS is increased to 60% for the curing conditions used. At this weight fraction only large macroscopic particles have been found to exist in the film.

When TEOS is reacted in the presence of PMMA and THF−0.l mL of DMF, the particles structure is determined early in the reaction as evidenced from the large initial radius of gyration as well as the large number of initial silicate sub-microscopic particles. These particles have structures dependent upon the initial TEOS weight fraction. In general the particles formed in a system containing DMF are larger than those formed in THF because of a higher condensation rate in the former, while the varying structure is believed to be the result of the limited amount of DMF used in the reaction.

Acknowledgment. The authors would like to acknowledge the financial support of the Office of Naval Research for this work.

CM960562A